1 Computational Analysis

Classical molecular dynamics simulations were performed to analyze the interface formed between various aqueous salt solutions and carbontetrachloride. Three salt solutions were simulated, as well as a reference system consisting of neat water for comparison to previous computational efforts.[1–6] The salts used in the simulations were NaCl, $NaNO_3$, and Na_2SO_4. These were chosen to compare to the experimental SFG results, and to supplement those experiments with additional molecular-level information. Analyses were performed on the simulation data to extract ionic and molecular density data, information about water coordination near to the interface, and water orientation data from order parameter analysis. The analyses are similar to, and logical extensions of previous computational work done on aqueous salt systems.

1.1 Density Profiles

Density histograms of simulated interfaces have been used in previous publications to show ionic and molecular distribution behavior in various systems.[2,4,6–11] In this work the density profile of water through the interface is fitted to a hyperbolic tangent function[10,12] as shown below:

$$\rho(z) = \frac{1}{2}(\rho_1 + \rho_2) - \frac{1}{2}(\rho_1 - \rho_2)\tanh\left(\frac{z - z_0}{d}\right) \tag{1}$$

Equation (1) relates the interfacial density, ρ, to the bulk densities of the two phases, ρ_1 and ρ_2, the location of the Gibb's dividing surface, z_0, and the interfacial width, d. The "90-10" thickness of the interface is related to the fitting parameter d by:

$$t = 2.197d \tag{2}$$

These measures of interfacial thickness provide a means of comparing the depths to which the water phase is affected by ions located at the interface. The density distributions of the salts depict concentration and depletion phenomena throughout the interfacial region, and also serve to illustrate ionic affinity within this region. Previous work has been performed on the air-water interface with various ions introduced, and each shows a particular level of interfacial affinity, with the more polar ions being the most interfacially active. We present the density distribution results below for the H_2O-CCl_4 interfaces studied. The density profiles of the different anionic species are fitted using a modified tanh() function that includes a gaussian function to more closely fit the concentration near the interface. The anion fitting function allows for a more direct comparison of location and peak width between the different systems.

$$\rho(z) = \frac{1}{2}(\rho_1 + \rho_2) - \frac{1}{2}(\rho_1 - \rho_2)\tanh\left(\frac{z - z_0}{d}\right) + ae^{-\frac{(x-b)^2}{2c^2}} \tag{3}$$

The gaussian function allows one to locate the anion peak height a, centered at an offset location b, with a width c.

1.2 Water Coordination

The coordination of water and distribution of the various coordination types was determined for each interfacial system. Water coordination refers to the hydrogen-bonding structure of water molecules, and is a measure of the number and type of bonds made. A simple naming scheme used to describe each type of water coordination have been developed previously,[4] and so that nomenclature will be used in this work. It has been established that certain bonding structures dominate in different regions of the interface, thus each of the water density profiles will be broken down further into component coordination types to show the areas in which the various types are most prevalent. The parameters used to define a hydrogen-bond are taken from a previous work by this group.[4] Analysis of water coordination profiles is valuable for comparison to experimental VSF results within the OH-bond stretching region of the vibrational spectrum. These give a molecular-level description of the composition of an interface, and show the various water bonding types that will contribute most to the VSF signal. Additionally, the results of this work are compared to previous studies on the air and salt water interfaces to establish differences due to the addition of an organic phase.

1.3 Order Parameters

One means of describing molecular orientation relative to a surface is by use of order parameters.[13] This technique has been applied to biaxial molecules such as water at organic interfaces,[2] and organic molecules to elucidate structuring within the interfacial region.[1] The results of this work show the two order parameters, S_1 and S_2, as functions of distance from the interface Gibbs dividing surface.

$$S_1 = \frac{1}{2}\left\langle 3\cos^2(\theta) - 1 \right\rangle \tag{4}$$

$$S_2 = \frac{\langle \sin(\theta)\cos(2\phi) \rangle}{\langle \sin(\theta) \rangle} \tag{5}$$

The order parameters are calculated from the euler angle values of the molecular "tilt" θ, and the "twist" ϕ. The order parameter distributions are further broken down to show the values for individual water coordination types for determination of orientational behavior of each.

2 Computational Methods

The molecular dynamics methods used in this work reproduce those from our previous computational efforts with some modifications described below.[1,2,4] All molecular dynamics simulations were carried out using the Amber 9 software package. The polarizable molecular model parameters are taken from previous works on similar systems.[7,14–17] The polarizable POL3 model was used for water molecules.[18] Fully polarizable models have been used in previous interface simulation studies because they are known to more accurately reproduce interfacial structure and free energy profiles.[19–22]

A total of 4 systems were simulated consisting of aqueous salt and CCl_4 phases. A slab geometry was used to produce two interface regions, the analyses of which were averaged.[1] The organic region was formed in a box 30-Å on a side with 169 CCl_4 molecules to reproduce standard temperature density of 1.59-$\frac{g}{mL}$. The aqueous region was formed in a box 30x30x60-Å, with the long axis labeled the z-axis. The number of water molecules and ions varied for each system in order to reproduce a density of 1.2-M. The specific populations of each molecule are listed in table 2. The organic and aqueous boxes were then joined to form a system 90-Å long with interface areas of 30x30-Å.

System	H_2O	Cation	Anion
Neat Water	1800	0	0
NaCl	1759	40	40
$NaNO_3$	1732	40	40
Na_2SO_4	1740	86	43

Table 1 — Aqueous molecule and ion numbers. Listed are the populations of each component for the 4 simulated aqueous phases. All systems were simulated at near 1.2-M salt concentrations.

The water, salts, and CCl_4 were each randomly packed into their respective boxes with a minimum packing distance of 2.4-Å. After joining the aqueous and organic phases and forming the two interfaces, the total system was energy minimized using a conjugate gradient method. Following minimization, the system was equilibrated at a constant temperature of 298-K with weak coupling to a heat bath for a period of 10-ns, using a simulation timestep of 1.0-fs. A non-bonded potential cutoff of 9.0-Å was used. Following equilibration the system was simulated with the same parameters for a further 10-ns with atomic position data recorded every 50-fs. This resulted in a total of 200,000 snapshots which were used in the data analysis.

3 Component Densities

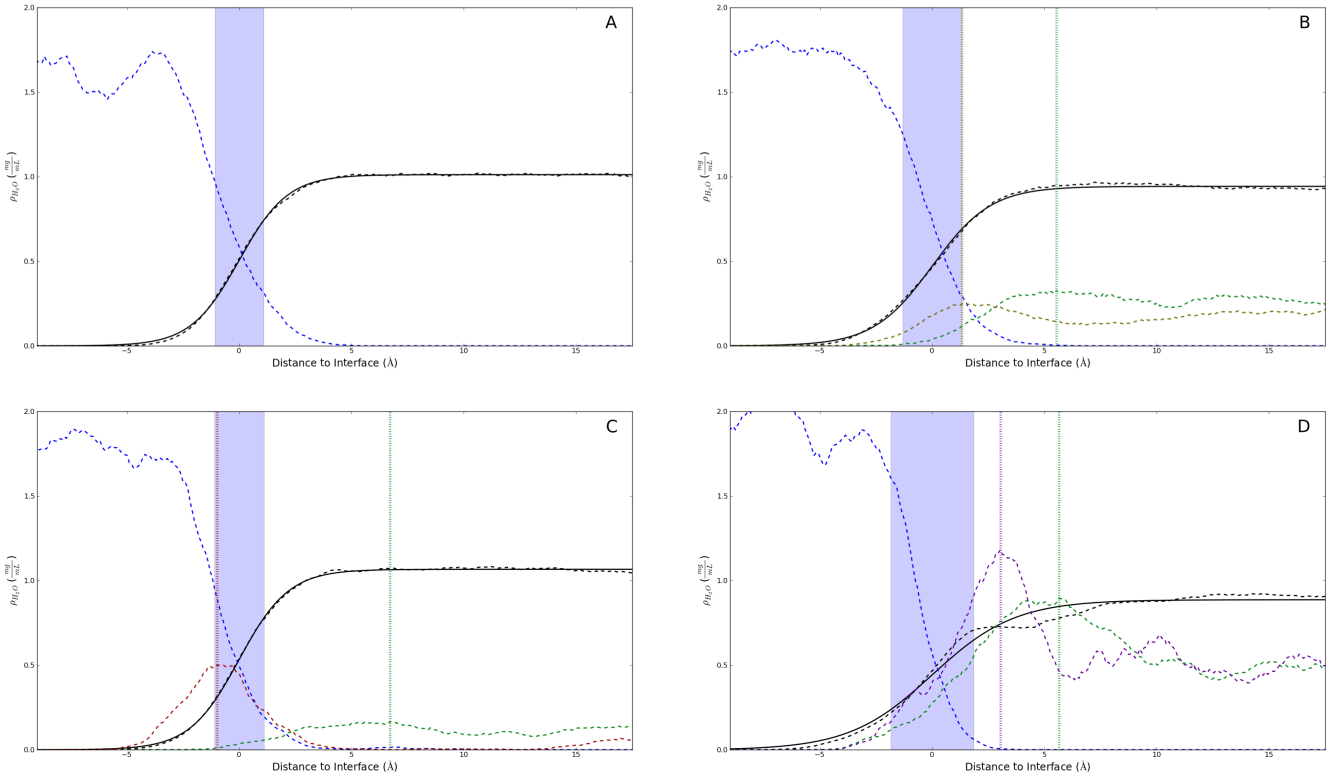

Figure. 1 — Aqueous salt and CCl_4 density profiles. The gibbs dividing surface location, z_0, were designated as the 0.0 $\mathring{A}$ location, and all lineshapes are plotted as distances to the gibbs interface. Neat-H_2O (A), NaCl (B), $NaNO_3$ (C), and Na_2SO_4 (D) salt-system densities are plotted with the water-oxygen density (dashed black) and the corresponding fitted lineshape (solid black). Each interfacial width, d, is designated as a highlighted blue region of width d centered about z_0. The CCl_4 (dashed blue), Na^+ cation (dashed green) and respective anion densities are also shown for each system. The scaling of the cation (10x) and anion (5x) densities was used to clarify their peak and trough locations. The maxima of the ionic components are marked with dashed vertical lines of the same colors to show relative component locations within the interfacial region.

The component density profiles of each system were calculated to quantify deviations from the neat-H_2O/CCl_4 system. The water density profile of each system was fitted to a hyperbolic tangent (Eq. 1), and the all the density profiles were plotted as distances from each of the gibbs dividing surface locations, z_0. The resulting plots are shown in figure 1 with letter labels that will be used to refer to the systems. z_0 of each system was shifted to a location of 0.0 $\mathring{A}$, and the interfacial thickness, d, is demarcated by a highlighted

region of the respective thickness centered about z_0. The thicknesses of the interfacial regions for the neat-H_2O (A), NaCl (B), $NaNO_3$ (C), and Na_2SO_4 (D) systems are 2.16, 2.62, 2.20, and 3.69 $\AA$ respectively. In each of the salt solutions, the peak in the anionic density profile occurs closer to the CCl_4 phase than the corresponding cationic peak. Various parameters of interest such as the interfacial thicknesses, ionic component locations, and relative distances between the peaks of the ion profiles are collected in table 2.

System	d	Anion	Cation	Anion-Cation Distance
Neat-H_2O	2.16	-	-	-
NaCl	2.62	1.33	5.53	4.20
$NaNO_3$	2.20	-0.99	6.71	7.70
Na_2SO_4	3.69	3.04	5.64	2.60

Table 2 — Aqueous salt system density parameters. Interfacial widths, d, and the locations of the maxima of the density profiles for each ionic component are listed for the simulated salt systems. The relative distances between the anion and cation density peak locations are listed to show how the different anions affect the relative location of their cationic counterions.

The fluctuations in the surface density profiles of water have been noted previously and attributed to thermal capillary waves on a larger length-scale than the system size.[23] The same work also made note that the interfacial thickness is size-dependent on the interfacial surface area. Increasing the surface area dimensions should cause an increase in the interfacial width. Two works on the water-CCl_4 surface offer direct comparison of this.[2,23] In comparing the interfacial widths, there is an increase in width as the system cross-sectional area is increased. This phenomenon implies that care must be taken when making quantitative comparisons between simulation studies.

Most of the recent studies on ion concentration near water interfaces have noted that large and polarizable ions will concentrate at the surface,[8,21,24,25] while small non-polarizable ion tend to be repelled. The surface enhancement calculated from molecular dynamics, however, portrays the lower bound of the actual effect because of the reduced polarizability values used in simulations to avoid the so-called "polarization catastrophe." The enhancement of surface anions is also believed to be the cause of the subsurface cation density increase. The counterions are attracted to the concentrations of anions at the surface, which are in turn stabilized by the increased polarization of the water due to the distorted interfacial electric field. The affinity for the surface follows the trend of surface tension increments, $\frac{d\gamma}{dm_2}$, where $Na_2SO_4 > NaCl > NaNO_3$.[24] This also follows the hoffmeister series trend for anions found to be the most "structure-making", and they are found to be enhanced further into the interface.

4 Water Orientation

5 Water Orientational Order Parameters

6 Calculated Sum-Frequency Spectra

References

1. Hore, D. K.; Walker, D. S.; MacKinnon, L.; Richmond, G. L. *Journal of Physical Chemistry C* **2007,** *111,* 8832-8842.

2. Hore, D. K.; Walker, D. S.; Richmond, G. L. *Journal of the American Chemical Society* **2008,** *130,* 1800+.

3. Hore, D. K.; Walker, D. S.; Richmond, G. L. *Journal of the American Chemical Society* **2007,** *129,* 752-753.

4. Walker, D. S.; Hore, D. K.; Richmond, G. L. *Journal of Physical Chemistry B* **2006,** *110,* 20451-20459.

5. Walker, D. S.; Richmond, G. L. *Journal of the American Chemical Society* **2007,** *129,* 9446-9451.

6. Walker, D. S.; Moore, F. G.; Richmond, G. L. *Journal of Physical Chemistry C* **2007,** *111,* 6103-6112.

7. Chang, T.; Peterson, K.; Dang, L. *Journal of Chemical Physics* **1995,** *103,* 7502-7513.

8. Eggimann, B. L.; Siepmann, J. I. *Journal of Physical Chemistry C* **2008,** *112,* 210-218.

9. Du, H.; Liu, J.; Ozdemir, O.; Nguyen, A. V.; Miller, J. D. *Journal of Colloid and Interface Science* **2008,** *318,* 271-277.

10. Wick, C.; Dang, L. *Journal of Physical Chemistry B* **2006,** *110,* 6824-6831.

11. Petersen, P.; Saykally, R.; Mucha, M.; Jungwirth, P. *Journal of Physical Chemistry B* **2005,** *109,* 10915-10921.

12. MATSUMOTO, M.; KATAOKA, Y. *Journal of Chemical Physics* **1988,** *88,* 3233-3245 hyperbolic tangent fitting function for water density profiles.

13. Buffeteau, T.; Labarthet, F.; Sourisseau, C.; Kostromine, S.; Bieringer, T. *MACROMOLECULES* **2004,** *37,* 2880-2889.

14. Chang, T.; Dang, L. *Journal of Physical Chemistry B* **1997,** *101,* 10518-10526.

15. Dang, L. *Journal of Physical Chemistry B* **1999,** *103,* 8195-8200.

16. Thomas, J. L.; Roeselova, M.; Dang, L. X.; Tobias, D. J. *Journal of Physical Chemistry A* **2007,** *111(16),* 3091-3098.

17. Hrobarik, T.; Vrbka, L.; Jungwirth, P. *BIOPHYSICAL CHEMISTRY* **2006,** *124,* 238-242.

18. Caldwell, J. W.; Kollman, P. A. *J. Phys. Chem.* **1995,** *99,* 6208-6219.

19. Rivera, J. L.; Starr, F. W.; Paricaud, P.; Cummings, P. T. *JOURNAL OF CHEMICAL PHYSICS* **2006,** *125,*.

20. Wick, C. D.; Kuo, I.-F. W.; Mundy, C. J.; Dang, L. X. *Journal of Chemical Theory and Computation* **2007,** *3,* 2002-2010.

21. Petersen, P.; Saykally, R. *Journal of the American Chemical Society* **2005,** *127,* 15446-15452.

22. Dang, L. *Journal of Physical Chemistry B* **1998,** *102,* 620-624.

23. Chang, T.; Dang, L. *Journal of Chemical Physics* **1996,** *104,* 6772-6783.

24. Pegram, L. M.; Record, Jr., M. T. *PROCEEDINGS OF THE NATIONAL ACADEMY OF SCIENCES OF THE UNITED STATES OF AMERICA* **2006,** *103,* 14278-14281.

25. Sloutskin, E.; Baumert, J.; Ocko, B. M.; Kuzmenko, I.; Checco, A.; Tamam, L.; Ofer, E.; Gog, T.; Gang, O.; Deutsch, M. *JOURNAL OF CHEMICAL PHYSICS* **2007,** *126,*.